The usage of GIS edge-approximation tools on vintage aerogeophysical data with focus on fault interpretation

Ingrid Schattauer (1), Esther Hintersberger (1), Christian Ullrich (2) Robert Supper (1) and Klaus Motschka (1)*

(1) Geological Survey of Austria (GBA), Neulinggasse 38, 1030 Vienna, Austria (2) Federal Office of Metrology and Surveying (BEV), Schiffamtsgasse 1-3, 1020 Vienna, Austria

Introduction

The reuse of vintage datasets (acquired in the 20th century) can pose challenges for modern geophysical modelling due to missing detailed preprocessing information, significant uncertainties or lack of precise tracking, etc. Nevertheless, they are often the only available datasets in a target region. We explore here the potential of such vintage airborne geophysical datasets (magnetics, AEM, radiometrics) to detect the location and dip direction of geological faults, using a non-modelling interpretation approach based on multiple edge-approximation GIS tools. We apply our approach in the eastern margin of the Bohemian Massif and the Lower Austrian Molasse basin between Krems and the Czech border. The applicability of the tools used in this study is evaluated based on the correlation of the identified lineaments with structures on the geological map.

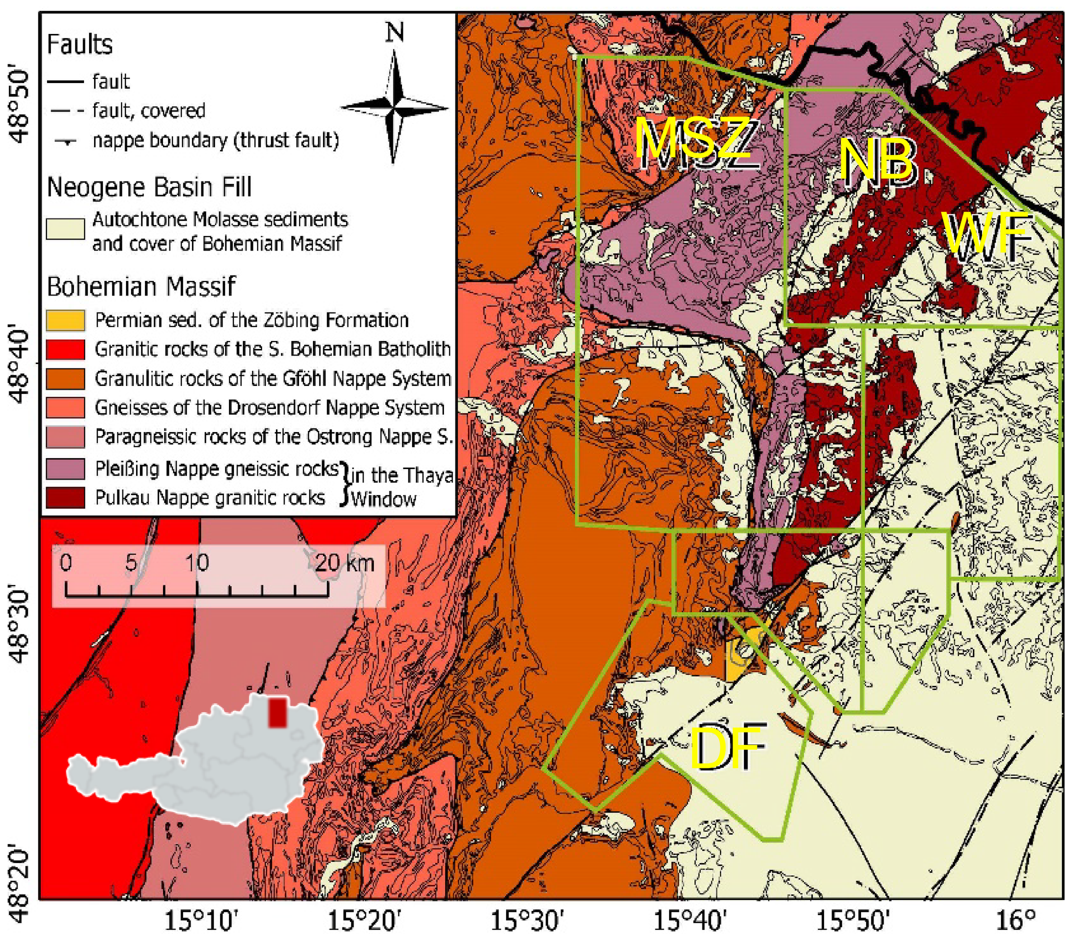

Fig: 1 Tectonic map of the study area, major faults considered in this study: DF – Diendorf Fault, MSZ – Moldanubian Shearzone, NB – Nappe boundary between Pleißing and Pulkau nappes within the Thaya Window, WF – Waitzendorf Fault. Green boxes show location of airborne datasets. Tectonic units based on the geological map of Lower Austria at the scale of 1:200.000 (Schnabel et al., 2002)

Vintage Aerogeophysical and Gravity data

Vintage aerogeophysical data has been acquired in several campaigns between 1983 and 1996, all data sets have been commonly reprocessed in 1998 (Supper, 1999).

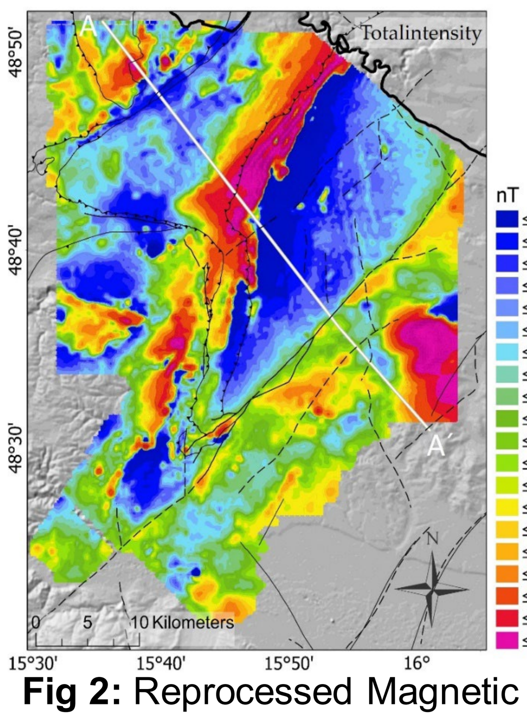

Fig 2: Reprocessed Magnetic Total intensity map [nT]

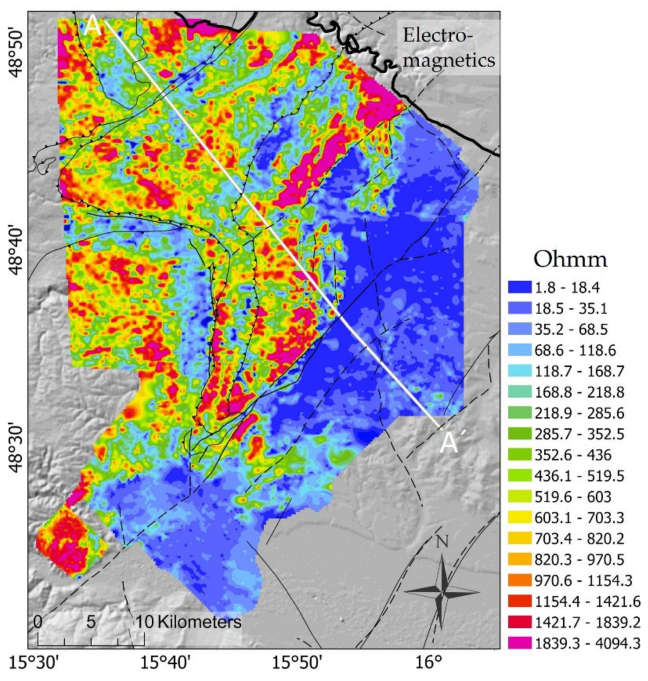

Fig 3: Apparent electrical resistivity map [Ohmm]

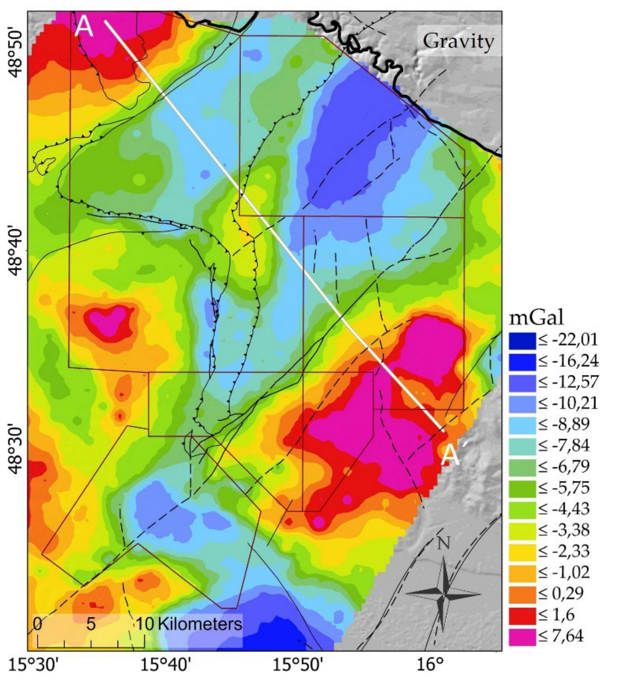

Fig 4: Bouguer anomaly map [mGal] based on the most recent data available at the BEV.

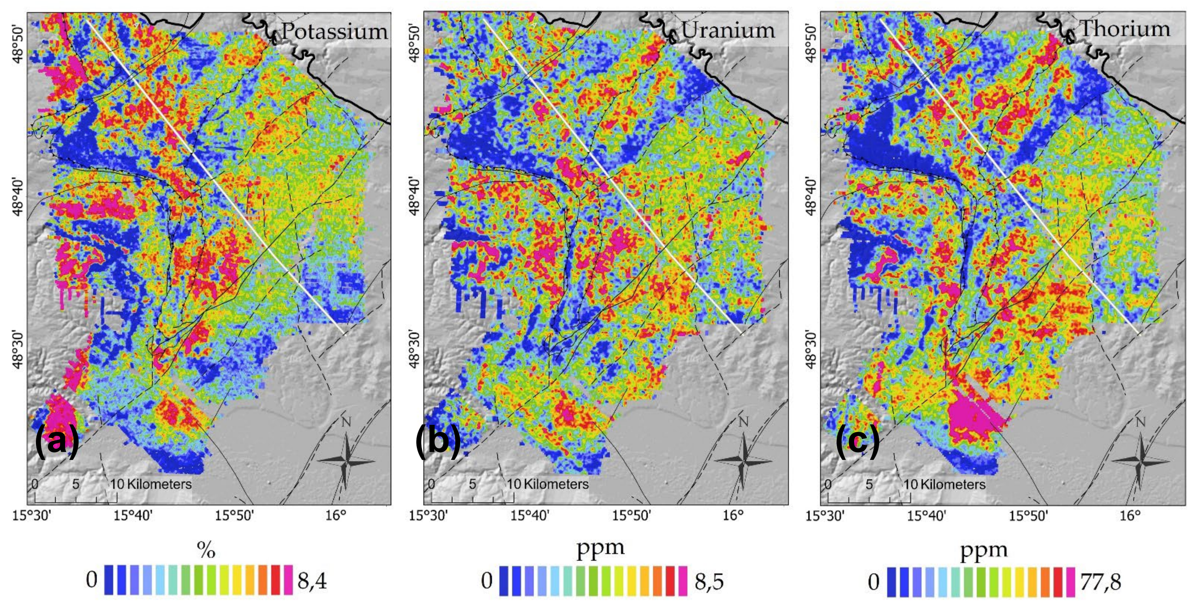

Fig 5: **(a)** Potassium map [%] **(b)** Uranium map [ppm] and **(c)** Thorium map [ppm]

Application of GIS tools for rapid fault interpretation

Raster to TIN

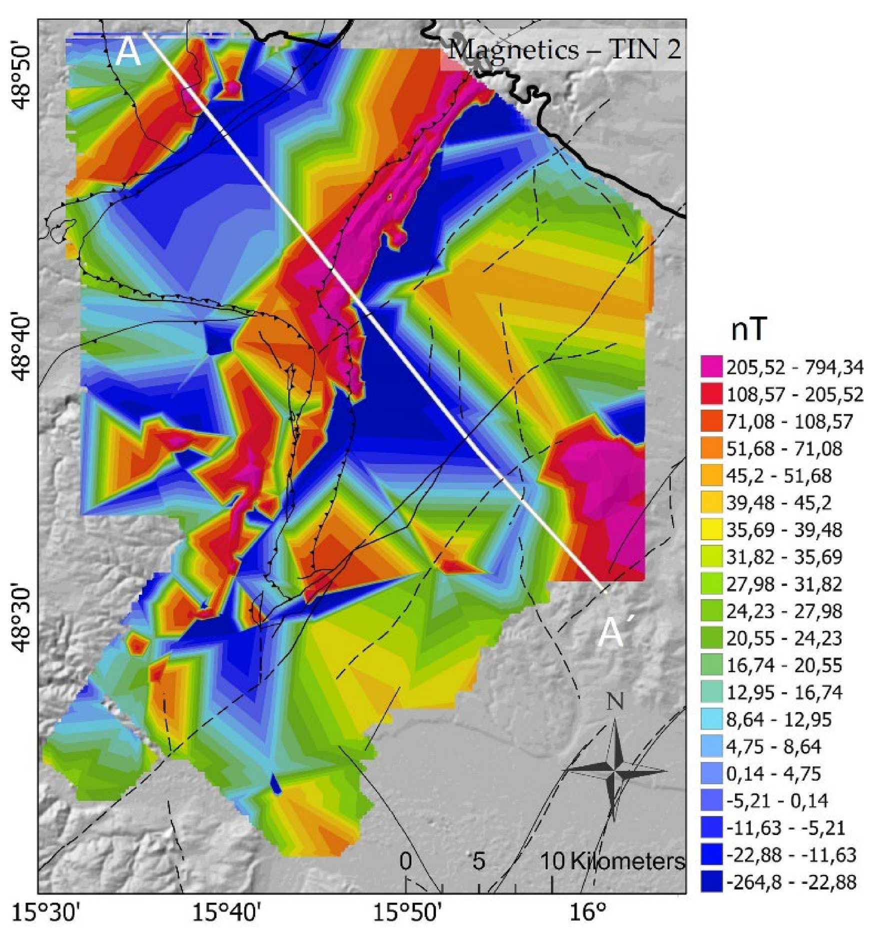

Fig 6: Magnetic total intensity - triangulated field with high z-tolerance (20 nT) and z-factor 20

Slope

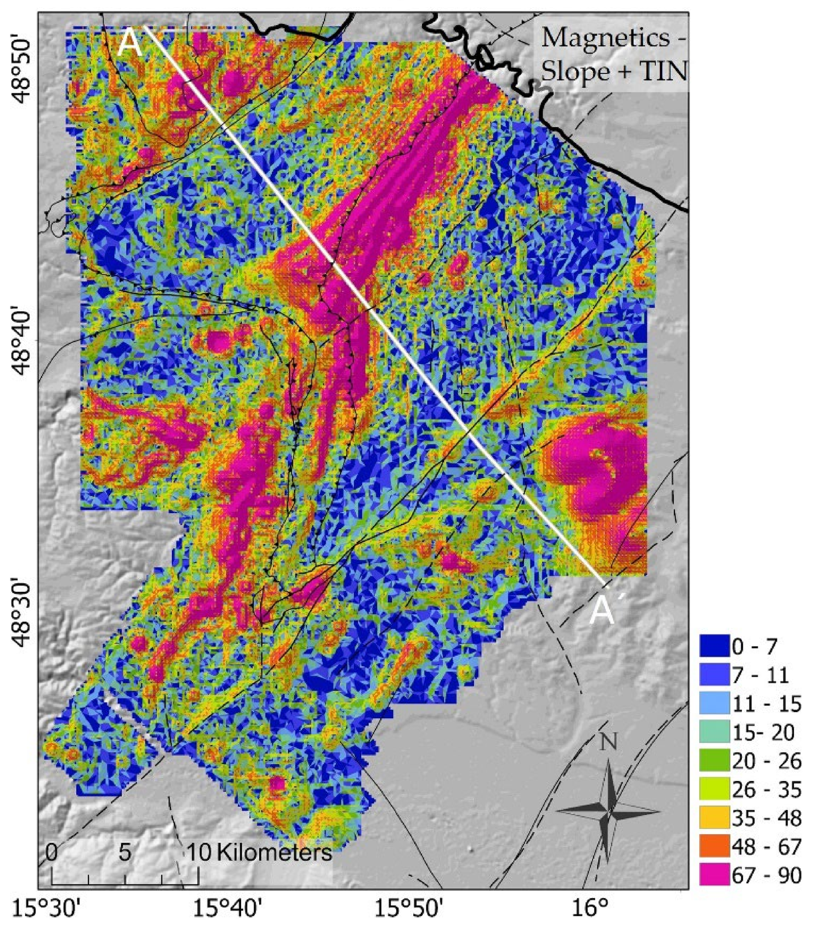

Fig 7: Slope amplitude [in degrees] of magnetic total intensity (triangulated field) with z- factor 20

Aspect-Slope

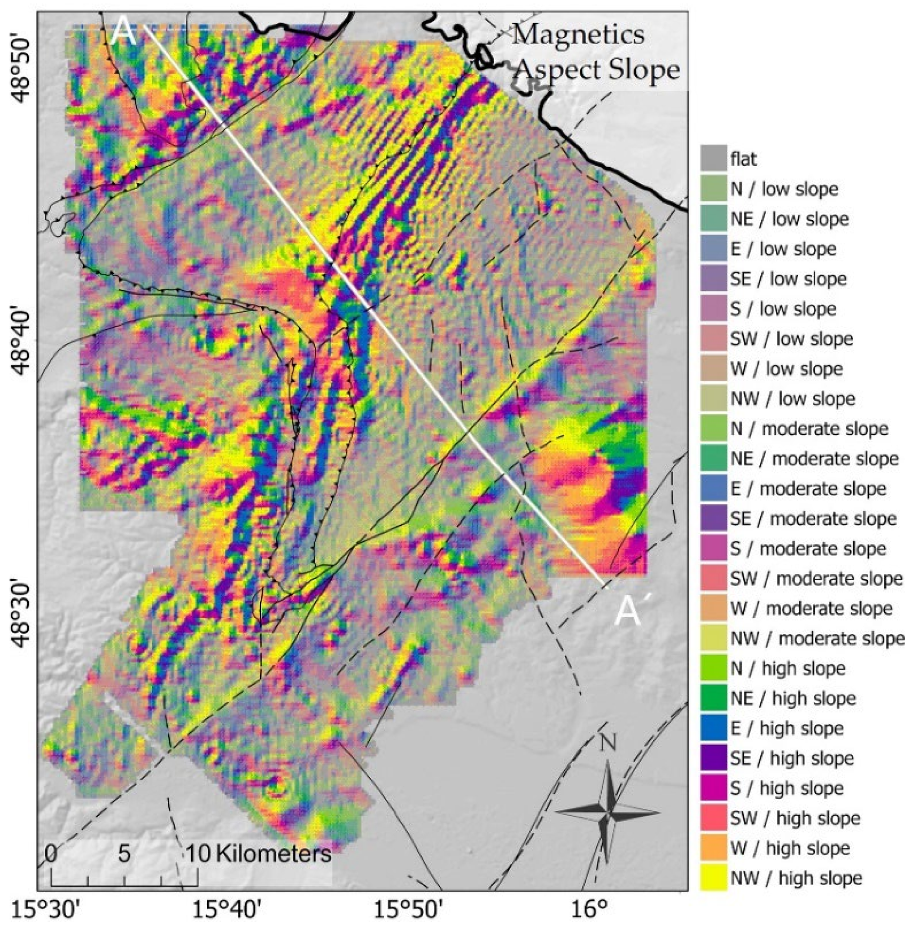

Fig 8: Aspect - slope applied to the magnetic total intensity with z-factor 10

Curvature

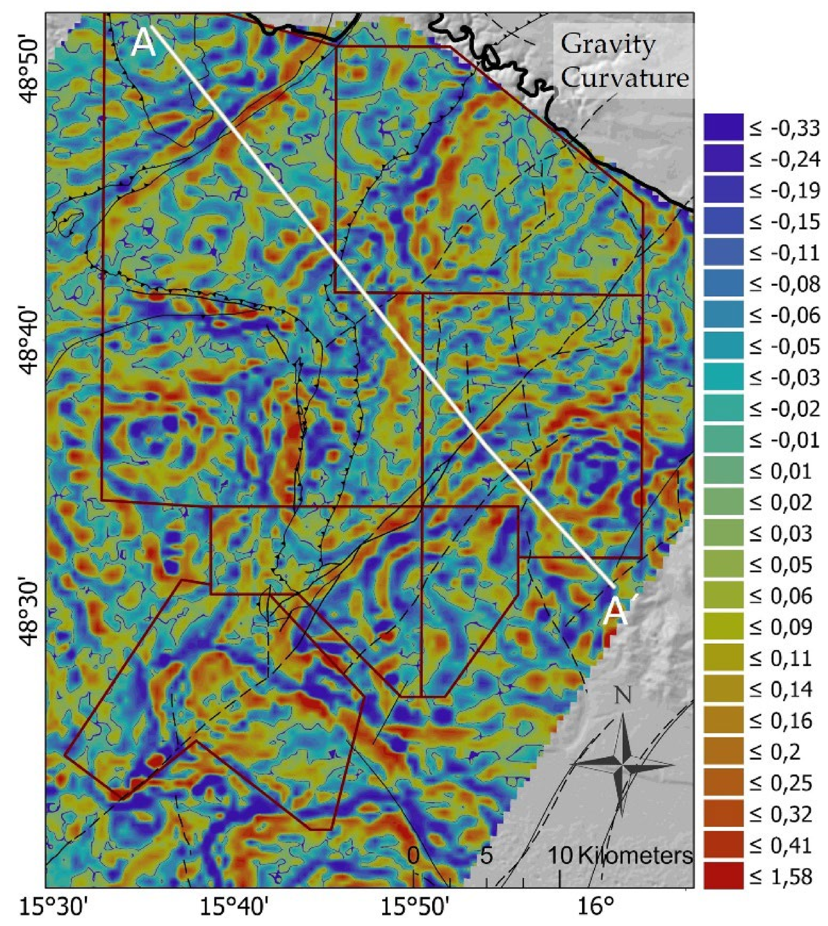

Fig 9: Profile curvature map of Bouguer anormaly data.

Comparison of methods

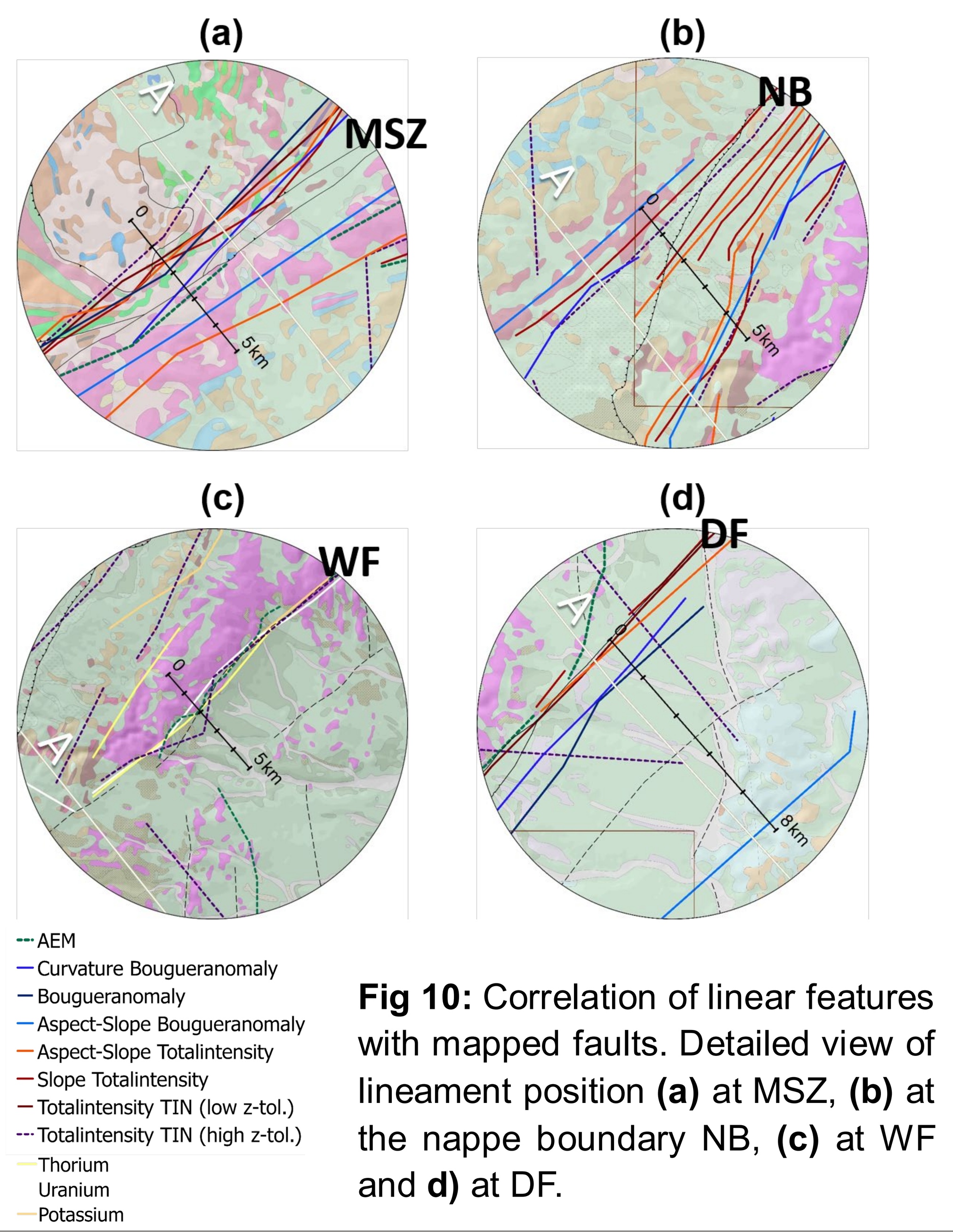

Fig 10: Correlation of linear features with mapped faults. Detailed view of lineament position **(a)** at MSZ, **(b)** at the nappe boundary NB, **(c)** at WF and **d)** at DF.

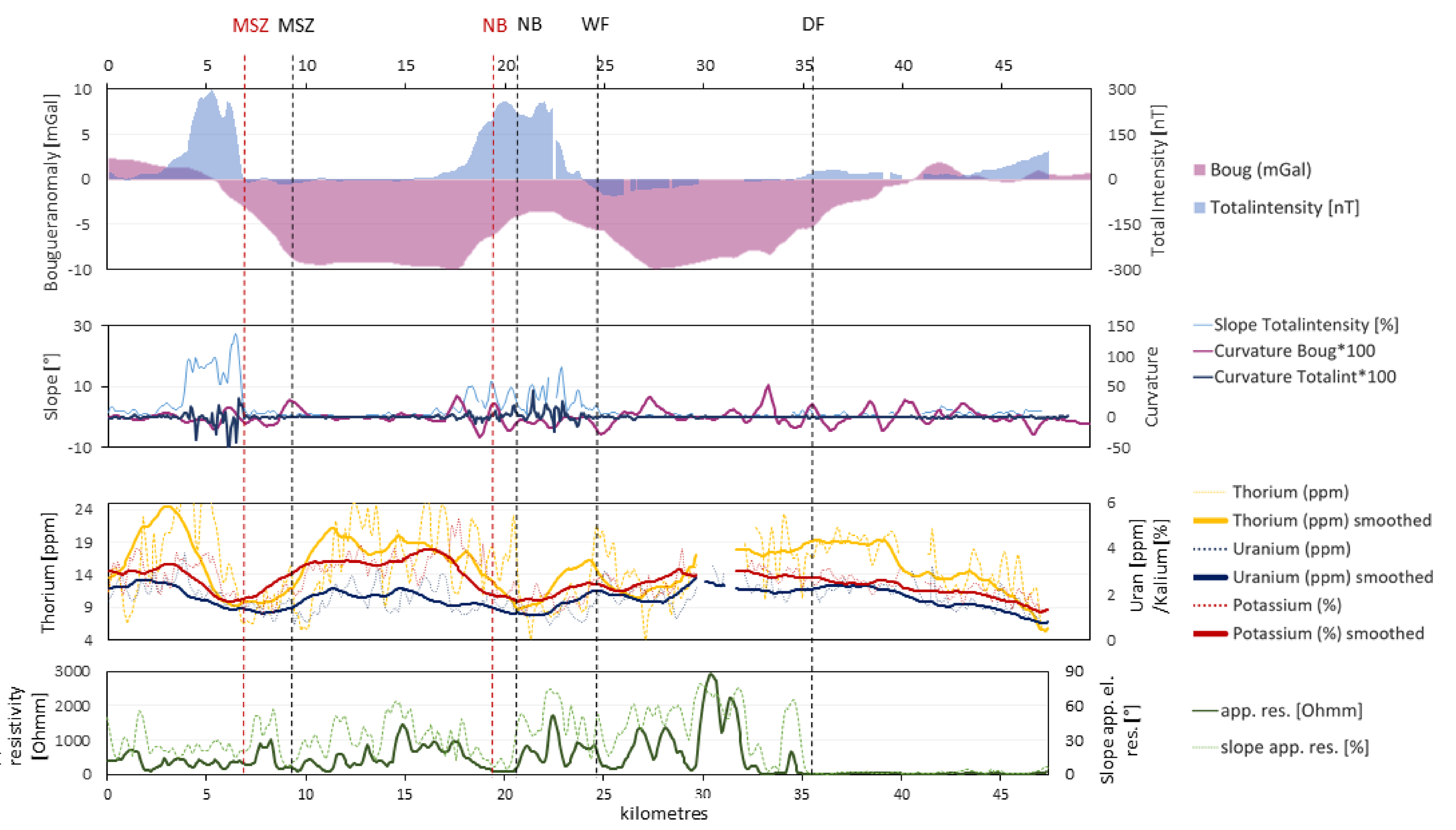

Fig 11: Comparison of different geophysical datasets and the respective derivations with the position of geological faults along profile A. Dashed black lines indicate fault position on geological map, red dashed line indicate proposed fault location at depth based on geophysical data

View	Method	field under consideration	tectonic structure MSZ	NB	WF	DF	applied key GIS-tool
Profile A	Gravity	Bougueranomaly (BA)	visible with limitations	visible with limitations	not visible	not visible	IDW
		Profile Curvature of BA	visible with limitations	not visible	visible with limitations	not visible	Profile Curvature
	Magnetics	Total Intensity (TI)	visible	not visible	visible with limitations	visible with limitations	IDW
		Slope of TI	visible	not visible	visible	visible with limitations	Slope
		Curvature of TI	visible	not visible	visible with limitations	not visible	Profile Curvature
	AEM	Apparent Resistivity	not visible	not visible	not visible	visible	IDW
	Radiometrics	Uranium	visible with limitations	not visible	visible with limitations	not visible	IDW
		Potassium	visible with limitations	visible with limitations	visible with limitations	not visible	IDW
		Thorium	visible with limitations	visible with limitations	visible with limitations	not visible	IDW
Map view	Gravity	Bougueranomaly	visible with limitations	not visible	not visible	visible with limitations	IDW
		Profile Curvature of BA	visible	not visible	not visible	visible with limitations	Profile Curvature
		Aspect Slope of BA	visible	visible with limitations	not visible	not visible	Aspect Slope
	Magnetics	Total Intensity (TI)	visible with limitations	not visible	not visible	visible	IDW
		TI TIN / low z - tol.	visible	not visible	not visible	visible	Raster to TIN
		TI TIN / high z - tol.	visible with limitations	not visible	visible	not visible	Raster to TIN
		Slope of TI	visible	not visible	not visible	visible	Raster to TIN / Slope
		Aspect slope of TI	visible	not visible	not visible	visible	Aspect Slope
	AEM	Apparent Resistivity	visible with limitations	not visible	visible	visible with limitations	IDW
	Radiometrics	Potassium	visible with limitations	visible with limitations	not visible	not visible	IDW
		Uranium	visible with limitations	not visible	visible	not visible	IDW
		Thorium	visible with limitations	not visible	visible	not visible	IDW

TIN=triangulated network
Magn. Intensity = Magnetization Intensity [A/m]
z - tol. = z Tolerance

visible | visible with limitations | not visible

Table 1 Summary of the interpreted results and an evaluation of their applicability to each of the major faults within the study area. MSZ = Moldanubian Shear Zone, NB = nappe boundary between Pulkau and Pleißing nappes, WF = Waitzendorf Fault, DF = Diendorf Fault.

GIS edge-approximation tools are useful for:

→ rapid data visualisation and interpretation
→ refinement of the understanding of tectonic structures
→ estimation whether geologic structures are buried or not
→ indication for vertical versus dipping fault geometries
→ application depends on geologic situation around the fault
→ combination of tools provides robust results
→ combination of tools provide information for different depths

More information soon available in the journal “Geoscience” (https://www.mdpi.com/journal/geosciences)

References:

Schnabel et al. (2002): Geologische Karte von Niederösterreich, 1:200.000

Supper, R. (1999): Auswertung aerogeophysikalischer Messungen im Bereich Niederösterreich Nord. Internal report. Geologische Bundesanstalt, Wien

This study was funded by the European Union's Horizon 2020 research and innovation programme and by the Bundesministerium für Bildung, Wissenschaft und Forschung

Bundesamt für Eich- und Vermessungswesen